

# Alternative pathways of dewetting for a thin two-layer film of soft matter

Andrey Pototsky, Michael Bestehorn, and Dominic Merkt

*Lehrstuhl für Theoretische Physik II,*

*Brandenburgische Technische Universität Cottbus,*

*Erich-Weinert-Straße 1, D-03046 Cottbus, Germany*

Uwe Thiele

*Max-Planck-Institut für Physik komplexer Systeme,*

*Nöthnitzer Straße 38, D-01187 Dresden, Germany*

## Abstract

We consider two stacked ultra-thin layers of different liquids on a solid substrate. Using long-wave theory, we derive coupled evolution equations for the free liquid-liquid and liquid-gas interfaces. Linear and non-linear analyses show that depending on the long-range van-der-Waals forces and the ratio of the layer thicknesses, the system follows different pathways of dewetting. The instability may be driven by varicose or zigzag modes and leads to film rupture either at the liquid-gas interface or at the substrate.

PACS numbers: 68.15.+e, 81.16.Rf, 68.55.-a, 47.20.Ky

Instability phenomena in ultra-thin soft matter films with thicknesses below 100 nm became relevant mainly because they obstruct the fabrication of homogeneous coatings [1]. The interest was further boosted by the possibility to control such processes and, to use them to manufacture functional layers on the nanometer scale [2, 3]. The stability of ultra-thin films is dominated by the effective molecular interactions between the substrate and the film surface [4]. They represent, for instance, long-range van-der-Waals forces which increase (decrease) the pressure in the film if they are attractive (repulsive) [5]. However, to determine the emerging length scale and pattern for unstable films a study of the film dynamics is required. Using a film thickness evolution equation obtained by long-wave approximation [6], the dewetting of a single layer of liquid is now reasonably well understood (see e.g. Ref. [7]).

However, little is known on the behaviour of two stacked ultra-thin layers of soft matter on a solid substrate (see Fig. 1). Such a two-layer film allows for richer dynamics than a one-layer system because, both, the free liquid-liquid and the free liquid-gas interface evolve in a coupled way. The evolution is driven by the effective molecular interactions between *all* the three interfaces separating the four material layers: substrate, liquid<sub>1</sub>, liquid<sub>2</sub> and ambient gas. Although experimental studies investigated different aspects of dewetting for two-layer films like interface instabilities or the growth of holes [8, 9, 10, 11, 12, 13, 14, 15] up to now no general theoretical description of the interface dynamics has been given. The case of small interface deflections was investigated in Ref. [16] for a thickness of the lower layer,  $d_1$ , much larger than that of the upper one ( $d_2 - d_1$ ). The most intricate question for the first stage of dewetting of a two-layer system is *which* interface will become unstable and *where* does the film rupture. This will determine the final morphology of the film. Experiments found roughening of the liquid-liquid interface [12] or an instability of the liquid-gas interface [8, 15]. Holes that evolve solely in the upper layer were also studied [9, 10].

In this Letter, we derive and analyse coupled long-wave evolution equations for the two interfaces that are valid for all interface deflections and thickness ratios. We show that solely by changing the relative thickness of the layers of soft matter one switches between different dominant instability modes. This leads to drastical changes of the pathway of dewetting from rupture at the substrate to rupture at the liquid-liquid interface (see Fig. 4 below). We illustrate our results for two-layer systems of polystyrene (PS) and polymethyl-metacrylate (PMMA) layers with silicon (Si) or silicon oxide (SiO) as substrate like studied

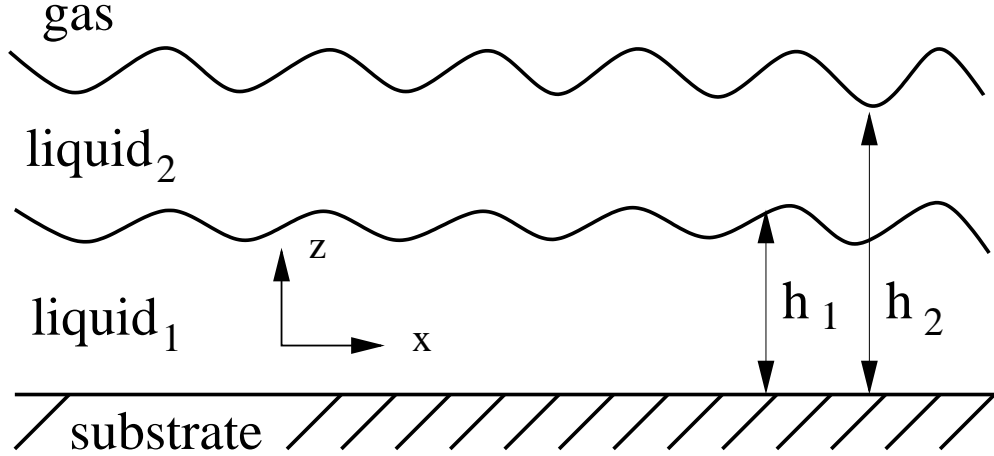


FIG. 1: Geometry of the two-layer system. The mean film thicknesses of the lower and upper layer are  $d_1$  and  $d_2 - d_1$ , respectively.

experimentally in Refs. [9, 11, 15].

We believe our model can be used not only for the description of the two-layer experiments, but also for a liquid film on a substrate with a stable but soft coating like a polymer brush [17] and, including driving terms, for studies of the transport of liquid droplets in liquid-liquid microfluidic systems [18].

*Coupled film thickness equations:* We obtain evolution equations for the film thicknesses  $h_1$  and  $h_2$  by simplifying the Navier-Stokes equations employing long-wave approximation [6]. Thereby a no-slip condition at the substrate, the continuity of the velocity field and the balance of the stress-tensors at the liquid-liquid and liquid-gas interfaces are used. Considering an isothermal two-layer system where both layer thicknesses are smaller than 100 nm, we neglect gravity and solely focus on the effective molecular interaction. For simplicity we only regard non-retarded long-range van-der-Waals forces resulting from dipole-dipole interactions between apolar materials. However, inclusion of other forces like e.g. short-range polar forces is straightforward as for one-layer films [19]. Details of the derivation will be presented elsewhere. We obtain

$$\begin{aligned}\frac{\partial h_1}{\partial t} &= \nabla \left( Q_{11} \nabla \frac{\delta F}{\delta h_1} + Q_{12} \nabla \frac{\delta F}{\delta h_2} \right) \\ \frac{\partial h_2}{\partial t} &= \nabla \left( Q_{21} \nabla \frac{\delta F}{\delta h_1} + Q_{22} \nabla \frac{\delta F}{\delta h_2} \right),\end{aligned}\quad (1)$$

where  $\delta F/\delta h_i$  with  $i = 1, 2$  denotes functional derivatives of the total energy of the system

$$F = \int [\rho_s + \rho_{vw}] dx \quad (2)$$

It contains the densities of the surface energy  $\rho_s = \frac{1}{2}[\sigma_1(\nabla h_1)^2 + \sigma_2(\nabla h_2)^2]$ , and of the energy for the van-der-Waals interaction  $\rho_{vw} = -A_{g21s}/(12\pi h_2^2) - A_{21s}/(12\pi h_1^2) - A_{12g}/[12\pi(h_2 - h_1)^2]$ . The surface tensions  $\sigma_1$  and  $\sigma_2$  belong to the liquid-liquid and liquid-gas interface, respectively.  $A_{g21s}$ ,  $A_{21s}$  and  $A_{12g}$  are four- and three-index Hamaker constants, with subscripts s, 1, 2 and g referring to the substrate, liquid<sub>1</sub>, liquid<sub>2</sub> and gas, respectively [20].

The symmetric matrix of the positive mobility factors  $Q_{ik}$  reads

$$\mathbf{Q} = \frac{1}{3\mu_1} \begin{pmatrix} h_1^3 & \frac{3h_1^2}{2} \left( h_2 - \frac{h_1}{3} \right) \\ \frac{3h_1^2}{2} \left( h_2 - \frac{h_1}{3} \right) & \frac{(h_2 - h_1)^3(\mu_1 - \mu_2)}{\mu_2} + h_2^3 \end{pmatrix} \quad (3)$$

where  $\mu_1$  and  $\mu_2$  are the viscosities of liquid<sub>1</sub> and liquid<sub>2</sub>, respectively. Note, that for  $d_2 - d_1 \ll d_1$  and for small surface deflections Eqs. (1) simplify to those of Ref. [16]. Assuming two identical liquids, Eqs. (1) reduces to the well known one-layer equation [6]. We non-dimensionalize Eqs. (1) by scaling  $\mathbf{x}$  with  $(d_2 - d_1)^2 \sqrt{2\pi\sigma_1/|A_{12g}|}$ ,  $h_i$  with  $d_2 - d_1$  and  $t$  with  $4\pi^2\mu_1\sigma_1(d_2 - d_1)^5/A_{12g}^2$ . The corresponding energy scale is  $|A_{12g}|/2\pi(d_2 - d_1)^2$ . The ratios of the mean thicknesses, surface tensions and viscosities are  $d = d_2/d_1$ ,  $\sigma = \sigma_2/\sigma_1$  and  $\mu = \mu_2/\mu_1$ , respectively.

We simulate the coupled time evolution of  $h_1$  and  $h_2$ , Eqs. (1), in a one-dimensional domain using a semi-implicit time integration scheme and periodic boundary conditions. Initial conditions consist of flat layers with an imposed noise of amplitude 0.001. Alternative pathways of dewetting that occur for different thickness ratios  $d$  are presented in Fig. 4 using a Si/PMMA/PS/air system as an example. Fig. 4 (a) shows that for a relatively small  $d = 1.4$  the two interfaces start to evolve deflections that are in anti-phase indicating the dominance of a varicose mode. When the liquid-gas interface approaches the liquid-liquid interface the latter starts to move downwards due to dynamical effects. This pathway leads to rupture of the upper layer, i.e. at the liquid-gas interface. On the contrary, Fig. 4 (b) shows that for a larger  $d = 2.4$  the growing deflections of the two interfaces are in phase indicating the dominance of a zigzag mode. As a consequence, here the lower layer ruptures, i.e. rupture occurs at the substrate.

*Linear stability analysis:* Deeper understanding of the different pathways can be reached by studying the linear stability of the initial flat layers. We linearize Eqs. (1) for small

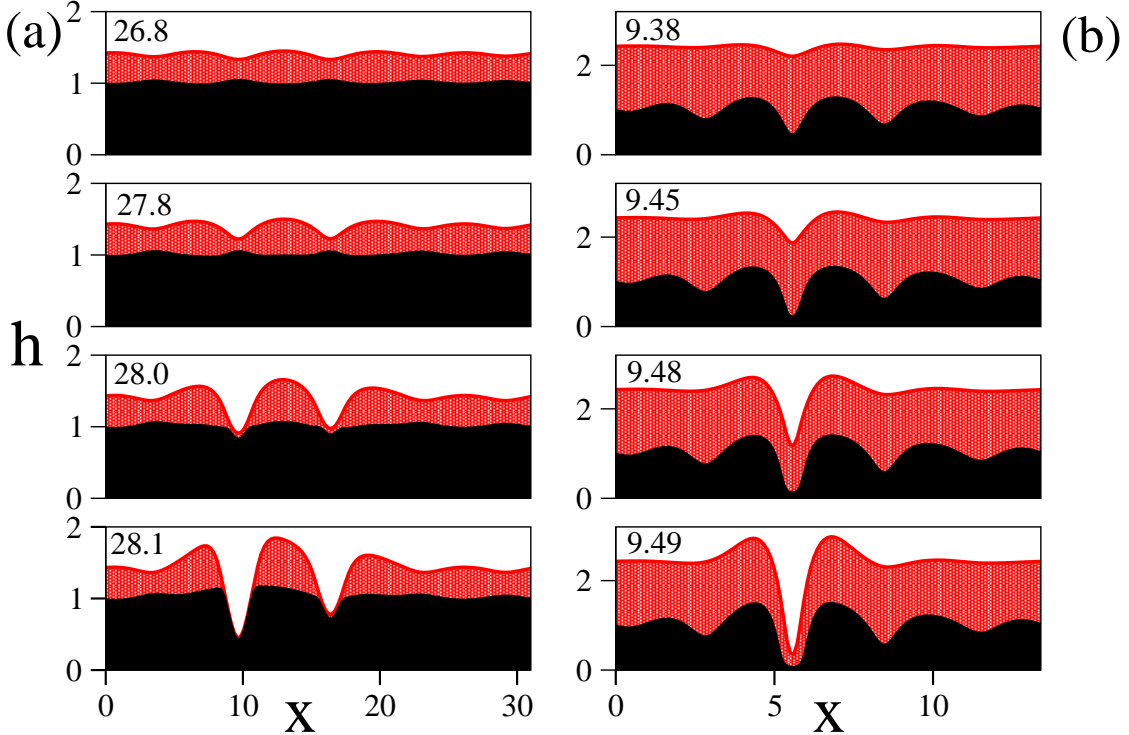


FIG. 2: Snapshots from time evolutions of a two-layer film for a Si/PMMA/PS/air system at dimensionless times as shown in the insets. (a) At  $d = 1.4$  a varicose mode evolves leading to rupture of the upper layer at the liquid-liquid interface. (b) At  $d = 2.4$  a zigzag mode evolves and rupture of the lower layer occurs at the substrate. The domain lengths are 5 times the corresponding fastest unstable wave length and  $\mu = \sigma = 1$ .

disturbances  $\chi_i \exp(\beta t) \cos(kx)$  for  $i = 1, 2$ , where  $k$ ,  $\beta$  and  $\chi_i$  are the wave number, growth rate and amplitudes of the disturbance, respectively. This leads to the eigenvalue problem  $(\mathbf{J} - \beta \mathbf{I})\boldsymbol{\chi} = 0$ , where  $\mathbf{J}$  is the *non-symmetric* Jacobi matrix with the eigenvector  $\boldsymbol{\chi} = (\chi_1, \chi_2)$ . We write  $\mathbf{J}$  as a product  $-k^2 \mathbf{Q} \cdot \mathbf{E}(k)$ , where  $\mathbf{Q}$  is the scaled symmetric mobility matrix and  $\mathbf{E}$  is the symmetric matrix of the scaled second variations of  $F$  (Eq. (2)) in Fourier space, i.e.  $E_{ij} = \partial_{h_i h_j} \rho_{VW} + \delta_{ij} \tilde{\sigma}_i k^2$  where  $\tilde{\sigma}_1 = 1$ ,  $\tilde{\sigma}_2 = \sigma$  and  $\delta_{ij} = 1$  for  $i = j$  and zero otherwise. For  $\det \mathbf{Q} \neq 0$  the eigenvalue problem can be written as a generalized eigenvalue problem:  $(k^2 \mathbf{E} + \beta \mathbf{Q}^{-1})\boldsymbol{\chi} = 0$ . With  $\mathbf{Q}$  also  $\mathbf{Q}^{-1}$  is positive definite and symmetric, ensuring all eigenvalues  $\beta$  to be real [21]. Inspection of the generalized eigenvalue problem shows that the stability is completely determined by the eigenvalues of  $\mathbf{E}$ . Since the surface tension terms are always positive, the stability threshold is found for  $k = 0$ , i.e. the system is linearly

stable for

$$\det \mathbf{E} > 0 \quad \text{and} \quad E_{11} > 0 \quad \text{at} \quad k = 0. \quad (4)$$

Fixing the coupling term  $\partial_{h_1 h_2} \rho_{VW}$ , the threshold is given by the positive hyperbole  $\partial_{h_2 h_2} \rho_{VW} = 1/\partial_{h_1 h_1} \rho_{VW}$  shown as solid line in Fig. 2. An instability sets in if at least one of the conditions (4) is violated. This implies, for instance, that the two-layer film can be unstable even if both,  $\partial_{h_1 h_1} \rho_{VW}$  and  $\partial_{h_2 h_2} \rho_{VW}$  are positive. The dashed line in Fig. 2 separates regions with one and two unstable eigenmodes, respectively. In the unstable region the growth rates are positive only for  $k$  smaller than the corresponding cut-off wavenumbers given by  $\det \mathbf{E}(k) = 0$ . One distinguishes two different types of unstable modes, namely,

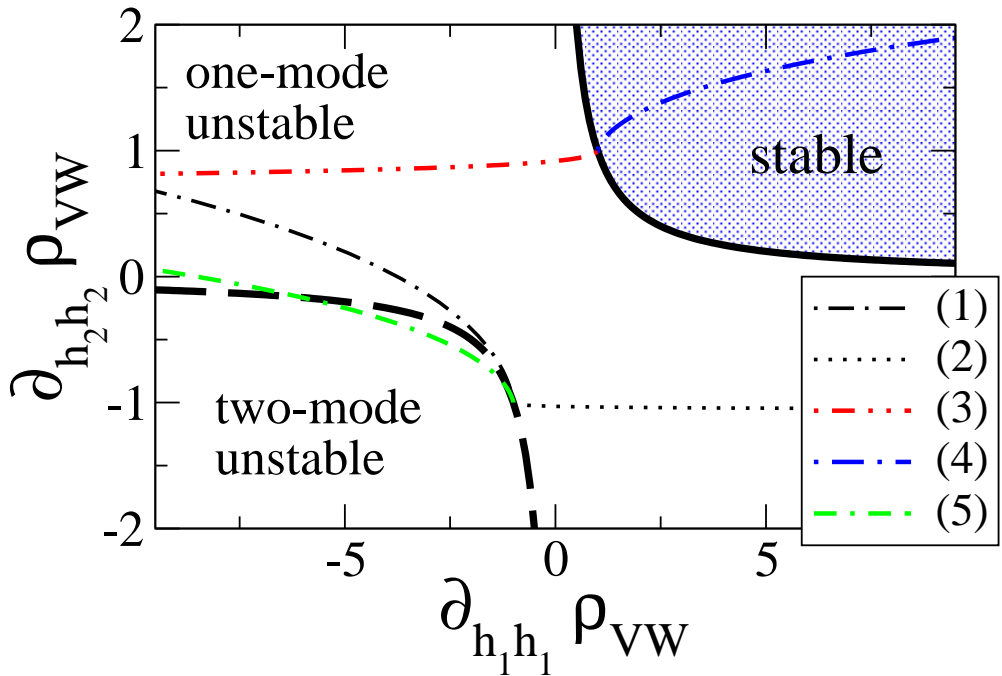


FIG. 3: Phase diagram for fixed scaled coupling  $\partial_{h_1 h_2} \rho_{VW} = A_{12g}/|A_{12g}|$ . Shown are the the stability threshold (solid line) and the boundary between unstable one-mode and two-mode regions (dashed line). The thin lines represent the trajectories for commonly studied systems: (1) Si/PMMA/PS/air, (2) SiO/PMMA/PS/air, (3) SiO/PS/PDMS/air, (4) Si/PS/PDMS/air, and (5) Si/PDMS/PS/air. The Hamaker constants were calculated as detailed below [20].

varicose and zigzag modes that also determine the non-linear evolution as discussed above (Fig. 4). Note, that the model in Ref. [16] gives only an unstable varicose mode, whereas in the general case also the zigzag mode can become unstable. Both modes are asymmetric

since the deflection amplitudes of the two interfaces are normally different. We characterize the asymmetry by the angle  $\phi = \arctan(\chi_1/\chi_2)$ , i.e. negative (positive)  $\phi$  correspond to varicose (zigzag) modes. The asymmetry increases with the ratio of the surface tensions  $\sigma$ . Note, that the dispersion relation and the type of the dominant mode depend on  $\sigma$  and  $\mu$ , whereas the stability diagram Fig. 2 *does not*. Fixing the Hamaker constants, i.e.

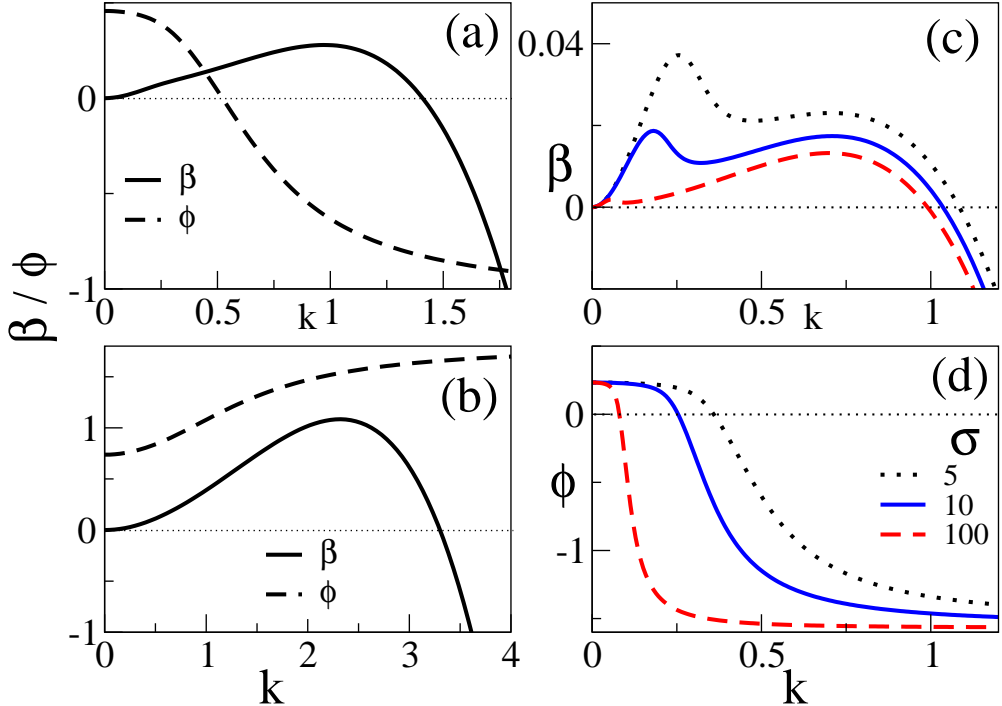


FIG. 4: Shown are the growth rate  $\beta$  and the corresponding angle  $\phi$  for the leading eigenmode. Panels (a) and (b) give an example for the one-mode varicose region at  $d = 1.4$  and (b) the one-mode zigzag region at  $d = 2.4$  for parameters as in Fig. 4. Panels (c) and (d) give  $\beta$  and  $\phi$ , respectively, for a SiO/PMMA/PS/air system at  $d = 2.16$  for  $\mu = 1$  and different  $\sigma$  as given in the inset of (d).

the combination of materials, and changing  $d$  one finds a line (trajectory) in the stability diagram Fig. 2 as shown for a variety of experimentally studied systems. Interestingly, for van-der-Waals interactions calculated as detailed in [20] one can show that such a trajectory *can not* cross the stability threshold, i.e. it is not possible to stabilize such a two-layer system by solely changing  $d$ . For instance, for the Si/PMMA/PS/air system the second condition in (4) is violated for all  $d$  and the system is always unstable. At  $d = 1$ , i.e. for vanishing upper layer, the system is on the boundary between the one- and the two-mode regions. For

$1 < d < 2.3$  the unstable mode is an asymmetric varicose mode, i.e. the angle  $\phi$  is negative at the maximum of the disperion relation  $\beta(k)$ . This is shown for  $d = 1.4$  in Fig. 3 (a) (cp. the time evolution in Fig. 4 (a)).

For  $d > 2.3$ , i.e. for smaller thicknesses of the lower layer, the unstable mode is an asymmetric zigzag mode. Fig. 3 (b) gives the dispersion relation  $\beta(k)$  and the angle  $\phi$  for  $d = 2.4$  corresponding to the time evolution shown in Fig. 4 (b). For the fastest mode  $\phi$  is close to  $\pi/2$ , i.e. the zigzag mode is strongly asymmetric - the deflection of the liquid-liquid interface dominates the linear stage of the evolution. Further on, the simultaneous action

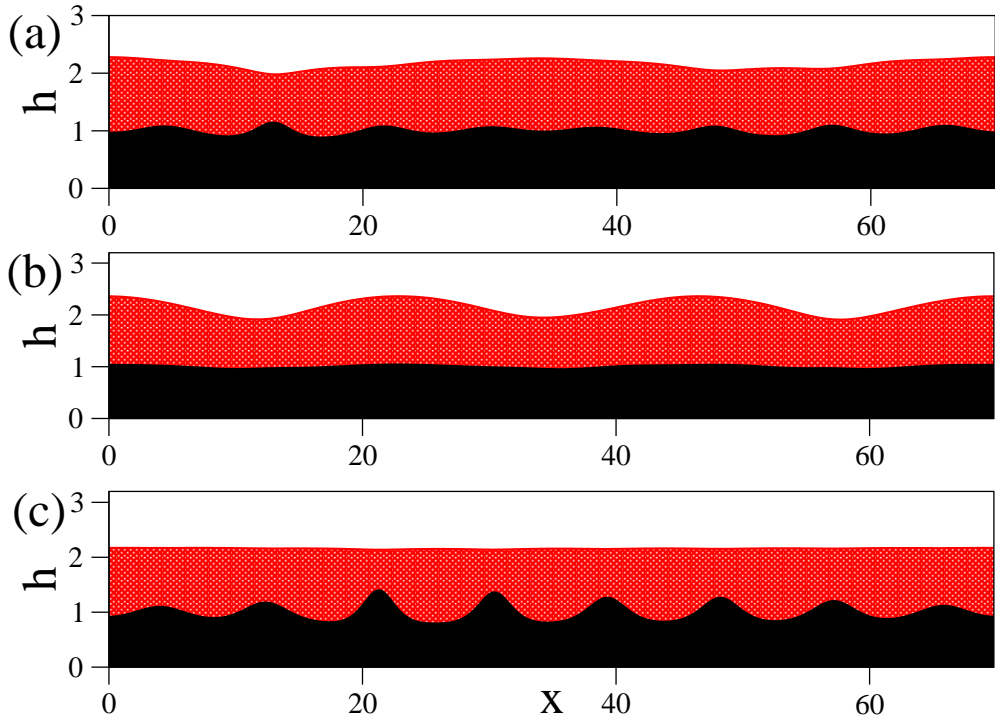


FIG. 5: Single snapshots from time evolutions of a SiO/PMMA/PS/air system for  $d = 2.16, \mu = 1$  and different  $\sigma$  corresponding to Fig. 3 (c) and (d). (a) The respective evolutions of the two interfaces are dominated by modes of different wavelength ( $\sigma = 10, t = 460$ ). In (b) and (c) the evolution of the entire two-layer system is dominated by the liquid-gas and the liquid-liquid interface, respectively ( $\sigma = 5, t = 234$  and  $\sigma = 100, t = 624$ ).

of the van-der-Waals forces between the three interfaces allows for dispersion relations with two maxima. An experimental system showing this unusual form of  $\beta(k)$  can be realized with a substrate that is less polarizable than both layers of soft matter. This is the case for the SiO/PMMA/PS/air system [20]. Dispersion relation and corresponding angle  $\phi$  are

shown for  $d = 2.16$  and different values of  $\sigma$  in Figs. 3 (c) and (d), respectively.

For the curves with two maxima the one at small  $k$  corresponds to a zigzag mode ( $\phi > 0$ ), whereas the one at large  $k$  corresponds to a varicose mode ( $\phi < 0$ ). The respective strong asymmetries of the two modes assure that the larger (smaller) wavelength will predominantly be seen at the liquid-gas (liquid-liquid) interface. This is illustrated by Fig. 5 where we show single snapshots from the non-linear time evolutions corresponding to the three dispersion relations shown in Fig. 3 (c) and (d).

In accordance with the linear analysis in Fig. 5 (a) the two interfaces are driven by different predominant modes resulting in different wave length. The instability of the liquid-gas interface is faster and has a larger wave length than the liquid-liquid interface. Finally, rupture occurs at the liquid-liquid interface (not shown). Solely changing the ratio of the surface tensions  $\sigma$  one can also find evolutions entirely dominated by the liquid-gas (Fig. 5 (b)) or the liquid-liquid (Fig. 5 (c)) interface, respectively.

To conclude, we have derived a system of coupled evolution equations for a thin two-layer film of soft matter driven by long-range van-der-Waals forces. Inclusion of other types of disjoining pressures is straightforward. The newly derived system represents the most general form of coupled evolution equations for two conserved order parameter fields in a relaxational situation and is apt to describe a broad variety of experimentally studied two-layer systems. Linear and non-linear analysis have shown that the mobilities have no influence on the stability threshold, but determine the length and time scales of the dynamics. We have shown for the first time that for a two-layer system *both* interface deflection modes - zigzag and varicose mode - may be unstable and lead to rupture at the substrate and the liquid-liquid interface, respectively.

---

- [1] G. Reiter, Phys. Rev. Lett. **68**, 75 (1992).
- [2] M. Mertig, U. Thiele, J. Bradt, D. Klemm, and W. Pompe, Appl. Phys. A **66**, S565 (1998).
- [3] U. Thiele, M. Mertig, and W. Pompe, Phys. Rev. Lett. **80**, 2869 (1998).
- [4] E. Ruckenstein and R. Jain, J. Chem. Soc. Faraday Trans. II **70**, 132 (1974).
- [5] J. N. Israelachvili, *Intermolecular and Surface Forces* (Academic Press, London, 1992).
- [6] A. Oron, S. H. Davis, and S. G. Bankoff, Rev. Mod. Phys. **69**, 931 (1997).

- [7] U. Thiele, Eur. Phys. J. E (2003), (in press), (2003).
- [8] A. Faldi, R. J. Composto, and K. I. Winey, Langmuir **11**, 4855 (1995).
- [9] P. Lambooy, K. C. Phelan, O. Haugg, and G. Krausch, Phys. Rev. Lett. **76**, 1110 (1996).
- [10] Q. Pan, K. I. Winey, H. H. Hu, and R. J. Composto, Langmuir **13**, 1758 (1997).
- [11] M. Sferrazza, C. Xiao, R. A. L. Jones, D. G. Bucknall, J. Webster, and J. Penfold, Phys. Rev. Lett. **78**, 3693 (1997).
- [12] M. Sferrazza, M. Heppenstall-Butler, R. Cubitt, D. Bucknall, J. Webster, and R. A. L. Jones, Phys. Rev. Lett. **81**, 5173 (1998).
- [13] M. O. David, G. Reiter, T. Sitthai, and J. Schultz, Langmuir **14**, 5667 (1998).
- [14] C. Renger, P. Müller-Buschbaum, M. Stamm, and G. Hinrichsen, Macromolecules **33**, 8388 (2000).
- [15] M. D. Morariu, E. Schäffer, and U. Steiner (unpublished).
- [16] F. Brochard-Wyart, P. Martin, and C. Redon, Langmuir **9**, 3682 (1993).
- [17] G. Reiter, J. Schultz, P. Auroy, and L. Auvray, Europhys. Lett. **33**, 29 (1996).
- [18] O. D. Velev, B. G. Prevo, and K. H. Bhatt, Science **426**, 515 (2003).
- [19] A. Sharma, Langmuir **9**, 861 (1993).
- [20] The four-index Hamaker constants are calculated using an equivalent of Eq. (11.13) of Ref. [5] that is based on the assumption that the main absorption frequencies of all involved media are about  $\nu = 3 \times 10^{15}$  Hz and that the zero frequency contribution is neglegtable. This yields

$$A_{ijkl} \approx \frac{3h\nu_e}{8\sqrt{2}} \frac{(n_i^2 - n_j^2)(n_l^2 - n_k^2)}{(n_i^2 + n_j^2)^{1/2}(n_l^2 + n_k^2)^{1/2}[(n_i^2 + n_j^2)^{1/2} + (n_l^2 + n_k^2)^{1/2}]}$$

The three-index Hamaker constants are obtained by  $A_{ijk} = A_{ijjk}$ . For the Si/PMMA/PS/air system one obtains  $A_{12g} = 1.49 \times 10^{-20}$  J,  $A_{21s} = 3.81 \times 10^{-20}$  J and  $A_{g21s} = -23.02 \times 10^{-20}$  J, whereas the SiO/PMMA/PS/air system is characterized by  $A_{12g} = 1.49 \times 10^{-20}$  J,  $A_{21s} = -0.02 \times 10^{-20}$  J and  $A_{g21s} = 0.15 \times 10^{-20}$  J. The used refractive indices of the media are  $n_{\text{PS}} = 1.59$ ,  $n_{\text{PDMS}} = 1.43$ ,  $n_{\text{PMMA}} = 1.49$ ,  $n_{\text{Si}} = 4.11$  and  $n_{\text{SiO}} = 1.48$  [15]. We generally neglect acoustic contributions to the disjoining pressure [22] because the accoustic modes are not confined to the individual liquid layers [15].

- [21] E. S. K. Manteuffel and K. Vettters, *Lineare Algebra* (Teubner Verlagsgesellschaft, Leipzig, 1987).
- [22] E. Schäffer and U. Steiner, Eur. Phys. J. E **8**, 347 (2002).